

Measurements of branching fraction, polarization, and charge asymmetry of $B^\pm \rightarrow \rho^\pm \rho^0$ and a search for $B^\pm \rightarrow \rho^\pm f_0(980)$

- B. Aubert,¹ M. Bona,¹ D. Boutigny,¹ F. Couderc,¹ Y. Karyotakis,¹ J. P. Lees,¹ V. Poireau,¹ V. Tisserand,¹ A. Zghiche,¹ E. Grauges,² A. Palano,³ J. C. Chen,⁴ N. D. Qi,⁴ G. Rong,⁴ P. Wang,⁴ Y. S. Zhu,⁴ G. Eigen,⁵ I. Ofte,⁵ B. Stugu,⁵ G. S. Abrams,⁶ M. Battaglia,⁶ D. N. Brown,⁶ J. Button-Shafer,⁶ R. N. Cahn,⁶ E. Charles,⁶ M. S. Gill,⁶ Y. Groysman,⁶ R. G. Jacobsen,⁶ J. A. Kadyk,⁶ L. T. Kerth,⁶ Yu. G. Kolomensky,⁶ G. Kukartsev,⁶ G. Lynch,⁶ L. M. Mir,⁶ T. J. Orikimoto,⁶ M. Pripstein,⁶ N. A. Roe,⁶ M. T. Ronan,⁶ W. A. Wenzel,⁶ P. del Amo Sanchez,⁷ M. Barrett,⁷ K. E. Ford,⁷ A. J. Hart,⁷ T. J. Harrison,⁷ C. M. Hawkes,⁷ A. T. Watson,⁷ T. Held,⁸ H. Koch,⁸ B. Lewandowski,⁸ M. Pelizaeus,⁸ K. Peters,⁸ T. Schroeder,⁸ M. Steinke,⁸ J. T. Boyd,⁹ J. P. Burke,⁹ W. N. Cottingham,⁹ D. Walker,⁹ D. J. Asgeirsson,¹⁰ T. Cuhadar-Donszelmann,¹⁰ B. G. Fulsom,¹⁰ C. Hearty,¹⁰ N. S. Knecht,¹⁰ T. S. Mattison,¹⁰ J. A. McKenna,¹⁰ A. Khan,¹¹ P. Kyberd,¹¹ M. Saleem,¹¹ D. J. Sherwood,¹¹ L. Teodorescu,¹¹ V. E. Blinov,¹² A. D. Bukin,¹² V. P. Druzhinin,¹² V. B. Golubev,¹² A. P. Onuchin,¹² S. I. Serednyakov,¹² Yu. I. Skovpen,¹² E. P. Solodov,¹² K. Yu Todyshev,¹² M. Bondioli,¹³ M. Bruinsma,¹³ M. Chao,¹³ S. Curry,¹³ I. Eschrich,¹³ D. Kirkby,¹³ A. J. Lankford,¹³ P. Lund,¹³ M. Mandelkern,¹³ R. K. Mommesen,¹³ W. Roethel,¹³ D. P. Stoker,¹³ S. Abachi,¹⁴ C. Buchanan,¹⁴ S. D. Foulkes,¹⁵ J. W. Gary,¹⁵ O. Long,¹⁵ B. C. Shen,¹⁵ K. Wang,¹⁵ L. Zhang,¹⁵ H. K. Hadavand,¹⁶ E. J. Hill,¹⁶ H. P. Paar,¹⁶ S. Rahatlou,¹⁶ V. Sharma,¹⁶ J. W. Berryhill,¹⁷ C. Campagnari,¹⁷ A. Cunha,¹⁷ B. Dahmes,¹⁷ T. M. Hong,¹⁷ D. Kovalskyi,¹⁷ J. D. Richman,¹⁷ T. W. Beck,¹⁸ A. M. Eisner,¹⁸ C. J. Flacco,¹⁸ C. A. Heusch,¹⁸ J. Kroeseberg,¹⁸ W. S. Lockman,¹⁸ G. Nesom,¹⁸ T. Schalk,¹⁸ B. A. Schumm,¹⁸ A. Seiden,¹⁸ P. Spradlin,¹⁸ D. C. Williams,¹⁸ M. G. Wilson,¹⁸ J. Albert,¹⁹ E. Chen,¹⁹ A. Dvoretskii,¹⁹ F. Fang,¹⁹ D. G. Hitlin,¹⁹ I. Narsky,¹⁹ T. Piatenko,¹⁹ F. C. Porter,¹⁹ A. Ryd,¹⁹ G. Mancinelli,²⁰ B. T. Meadows,²⁰ K. Mishra,²⁰ M. D. Sokoloff,²⁰ F. Blanc,²¹ P. C. Bloom,²¹ S. Chen,²¹ W. T. Ford,²¹ J. F. Hirschauer,²¹ A. Kreisel,²¹ M. Nagel,²¹ U. Nauenberg,²¹ A. Olivas,²¹ W. O. Ruddick,²¹ J. G. Smith,²¹ K. A. Ulmer,²¹ S. R. Wagner,²¹ J. Zhang,²¹ A. Chen,²² E. A. Eckhart,²² A. Soffer,²² W. H. Toki,²² R. J. Wilson,²² F. Winkelmeier,²² Q. Zeng,²² D. D. Altenburg,²³ E. Feltresi,²³ A. Hauke,²³ H. Jasper,²³ J. Merkel,²³ A. Petzold,²³ B. Spaan,²³ T. Brandt,²⁴ V. Klose,²⁴ H. M. Lacker,²⁴ W. F. Mader,²⁴ R. Nogowski,²⁴ J. Schubert,²⁴ K. R. Schubert,²⁴ R. Schwierz,²⁴ J. E. Sundermann,²⁴ A. Volk,²⁴ D. Bernard,²⁵ G. R. Bonneau,²⁵ E. Latour,²⁵ Ch. Thiebaux,²⁵ M. Verderi,²⁵ P. J. Clark,²⁶ W. Gradl,²⁶ F. Muheim,²⁶ S. Playfer,²⁶ A. I. Robertson,²⁶ Y. Xie,²⁶ M. Andreotti,²⁷ D. Bettoni,²⁷ C. Bozzi,²⁷ R. Calabrese,²⁷ G. Cibinetto,²⁷ E. Luppi,²⁷ M. Negrini,²⁷ A. Petrella,²⁷ L. Piemontese,²⁷ E. Prencipe,²⁷ F. Anulli,²⁸ R. Baldini-Ferroli,²⁸ A. Calcaterra,²⁸ R. de Sangro,²⁸ G. Finocchiaro,²⁸ S. Pacetti,²⁸ P. Patteri,²⁸ I. M. Peruzzi,^{28,*} M. Piccolo,²⁸ M. Rama,²⁸ A. Zallo,²⁸ A. Buzzo,²⁹ R. Contri,²⁹ M. Lo Vetere,²⁹ M. M. Macri,²⁹ M. R. Monge,²⁹ S. Passaggio,²⁹ C. Patrignani,²⁹ E. Robutti,²⁹ A. Santroni,²⁹ S. Tosi,²⁹ G. Brandenburg,³⁰ K. S. Chaisanguanthum,³⁰ M. Morii,³⁰ J. Wu,³⁰ R. S. Dubitzky,³¹ J. Marks,³¹ S. Schenck,³¹ U. Uwer,³¹ D. J. Bard,³² W. Bhimji,³² D. A. Bowerman,³² P. D. Dauncey,³² U. Egede,³² R. L. Flack,³² J. A. Nash,³² M. B. Nikolich,³² W. Panduro Vazquez,³² D. J. Bard,³³ P. K. Behera,³³ X. Chai,³³ M. J. Charles,³³ U. Mallik,³³ N. T. Meyer,³³ V. Ziegler,³³ J. Cochran,³⁴ H. B. Crawley,³⁴ L. Dong,³⁴ V. Eyges,³⁴ W. T. Meyer,³⁴ S. Prelle,³⁴ E. I. Rosenberg,³⁴ A. E. Rubin,³⁴ A. V. Gritsan,³⁵ A. G. Denig,³⁶ M. Fritsch,³⁶ G. Schott,³⁶ N. Arnaud,³⁷ M. Davier,³⁷ G. Grosdidier,³⁷ A. Höcker,³⁷ F. Le Diberder,³⁷ V. Lepeltier,³⁷ A. M. Lutz,³⁷ A. Oyanguren,³⁷ S. Pruvot,³⁷ S. Rodier,³⁷ P. Roudeau,³⁷ M. H. Schune,³⁷ A. Stocchi,³⁷ W. F. Wang,³⁷ G. Wormser,³⁷ C. H. Cheng,³⁸ D. J. Lange,³⁸ D. M. Wright,³⁸ C. A. Chavez,³⁹ I. J. Forster,³⁹ J. R. Fry,³⁹ E. Gabathuler,³⁹ R. Gamet,³⁹ K. A. George,³⁹ D. E. Hutchcroft,³⁹ D. J. Payne,³⁹ K. C. Schofield,³⁹ C. Touramanis,³⁹ A. J. Bevan,⁴⁰ F. Di Lodovico,⁴⁰ W. Menges,⁴⁰ R. Sacco,⁴⁰ G. Cowan,⁴¹ H. U. Flaecher,⁴¹ D. A. Hopkins,⁴¹ P. S. Jackson,⁴¹ T. R. McMahon,⁴¹ S. Ricciardi,⁴¹ F. Salvatore,⁴¹ A. C. Wren,⁴¹ D. N. Brown,⁴² C. L. Davis,⁴² J. Allison,⁴³ N. R. Barlow,⁴³ R. J. Barlow,⁴³ Y. M. Chia,⁴³ C. L. Edgar,⁴³ G. D. Lafferty,⁴³ M. T. Naisbit,⁴³ J. C. Williams,⁴³ J. I. Yi,⁴³ C. Chen,⁴⁴ W. D. Hulsbergen,⁴⁴ A. Jawahery,⁴⁴ C. K. Lae,⁴⁴ D. A. Roberts,⁴⁴ G. Simi,⁴⁴ G. Blaylock,⁴⁵ C. Dallapiccola,⁴⁵ S. S. Hertzbach,⁴⁵ X. Li,⁴⁵ T. B. Moore,⁴⁵ S. Saremi,⁴⁵ H. Staengle,⁴⁵ R. Cowan,⁴⁶ G. Sciolla,⁴⁶ S. J. Sekula,⁴⁶ M. Spitznagel,⁴⁶ F. Taylor,⁴⁶ R. K. Yamamoto,⁴⁶ H. Kim,⁴⁷ S. E. McLachlin,⁴⁷ P. M. Patel,⁴⁷ S. H. Robertson,⁴⁷ A. Lazzaro,⁴⁸ V. Lombardo,⁴⁸ F. Palombo,⁴⁸ J. M. Bauer,⁴⁹ L. Cremaldi,⁴⁹ V. Eschenburg,⁴⁹ R. Godang,⁴⁹ R. Kroeger,⁴⁹ D. A. Sanders,⁴⁹ D. J. Summers,⁴⁹ H. W. Zhao,⁴⁹ S. Brunet,⁵⁰ D. Côté,⁵⁰ M. Simard,⁵⁰ P. Taras,⁵⁰ F. B. Viaud,⁵⁰ H. Nicholson,⁵¹ N. Cavallo,^{52,†} G. De Nardo,⁵² F. Fabozzi,^{52,†} C. Gatto,⁵² L. Lista,⁵² D. Monorchio,⁵² P. Paolucci,⁵² D. Piccolo,⁵² C. Sciacca,⁵² M. A. Baak,⁵³ G. Raven,⁵³ H. L. Snoek,⁵³ C. P. Jessop,⁵⁴

J. M. LoSecco,⁵⁴ T. Allmendinger,⁵⁵ G. Benelli,⁵⁵ L. A. Corwin,⁵⁵ K. K. Gan,⁵⁵ K. Honscheid,⁵⁵ D. Hufnagel,⁵⁵ P. D. Jackson,⁵⁵ H. Kagan,⁵⁵ R. Kass,⁵⁵ A. M. Rahimi,⁵⁵ J. J. Regensburger,⁵⁵ R. Ter-Antonyan,⁵⁵ Q. K. Wong,⁵⁵ N. L. Blount,⁵⁶ J. Brau,⁵⁶ R. Frey,⁵⁶ O. Igonkina,⁵⁶ J. A. Kolb,⁵⁶ M. Lu,⁵⁶ R. Rahmat,⁵⁶ N. B. Sinev,⁵⁶ D. Strom,⁵⁶ J. Strube,⁵⁶ E. Torrence,⁵⁶ A. Gaz,⁵⁷ M. Margoni,⁵⁷ M. Morandin,⁵⁷ A. Pompili,⁵⁷ M. Posocco,⁵⁷ M. Rotondo,⁵⁷ F. Simonetto,⁵⁷ R. Stroili,⁵⁷ C. Voci,⁵⁷ M. Benayoun,⁵⁸ H. Briand,⁵⁸ J. Chauveau,⁵⁸ P. David,⁵⁸ L. Del Buono,⁵⁸ Ch. de la Vaissière,⁵⁸ O. Hamon,⁵⁸ B. L. Hartfiel,⁵⁸ Ph. Leruste,⁵⁸ J. Malclès,⁵⁸ J. Ocariz,⁵⁸ L. Roos,⁵⁸ G. Therin,⁵⁸ L. Gladney,⁵⁹ M. Biasini,⁶⁰ R. Covarelli,⁶⁰ C. Angelini,⁶¹ G. Batignani,⁶¹ S. Bettarini,⁶¹ F. Bucci,⁶¹ G. Calderini,⁶¹ M. Carpinelli,⁶¹ R. Cenci,⁶¹ F. Forti,⁶¹ M. A. Giorgi,⁶¹ A. Lusiani,⁶¹ G. Marchiori,⁶¹ M. A. Mazur,⁶¹ M. Morganti,⁶¹ N. Neri,⁶¹ E. Paoloni,⁶¹ G. Rizzo,⁶¹ J. J. Walsh,⁶¹ M. Haire,⁶² D. Judd,⁶² D. E. Wagoner,⁶² J. Biesiada,⁶³ N. Danielson,⁶³ P. Elmer,⁶³ Y. P. Lau,⁶³ C. Lu,⁶³ J. Olsen,⁶³ A. J. S. Smith,⁶³ A. V. Telnov,⁶³ F. Bellini,⁶⁴ G. Cavoto,⁶⁴ A. D'Orazio,⁶⁴ D. del Re,⁶⁴ E. Di Marco,⁶⁴ R. Faccini,⁶⁴ F. Ferrarotto,⁶⁴ F. Ferroni,⁶⁴ M. Gaspero,⁶⁴ L. Li Gioi,⁶⁴ M. A. Mazzoni,⁶⁴ S. Morganti,⁶⁴ G. Piredda,⁶⁴ F. Polci,⁶⁴ F. Safai Tehrani,⁶⁴ C. Voena,⁶⁴ M. Ebert,⁶⁵ H. Schröder,⁶⁵ R. Waldi,⁶⁵ T. Adye,⁶⁶ N. De Groot,⁶⁶ B. Franek,⁶⁶ E. O. Olaiya,⁶⁶ F. F. Wilson,⁶⁶ R. Aleksan,⁶⁷ S. Emery,⁶⁷ A. Gaidot,⁶⁷ S. F. Ganzhur,⁶⁷ G. Hamel de Monchenault,⁶⁷ W. Kozanecki,⁶⁷ M. Legendre,⁶⁷ G. Vasseur,⁶⁷ Ch. Yèche,⁶⁷ M. Zito,⁶⁷ X. R. Chen,⁶⁸ H. Liu,⁶⁸ W. Park,⁶⁸ M. V. Purohit,⁶⁸ J. R. Wilson,⁶⁸ M. T. Allen,⁶⁹ D. Aston,⁶⁹ R. Bartoldus,⁶⁹ P. Bechtle,⁶⁹ N. Berger,⁶⁹ R. Claus,⁶⁹ J. P. Coleman,⁶⁹ M. R. Convery,⁶⁹ M. Cristinziani,⁶⁹ J. C. Dingfelder,⁶⁹ J. Dorfan,⁶⁹ G. P. Dubois-Felsmann,⁶⁹ D. Dujmic,⁶⁹ W. Dunwoodie,⁶⁹ R. C. Field,⁶⁹ T. Glanzman,⁶⁹ S. J. Gowdy,⁶⁹ M. T. Graham,⁶⁹ P. Grenier,⁶⁹ V. Halyo,⁶⁹ C. Hast,⁶⁹ T. Hryna'ova,⁶⁹ W. R. Innes,⁶⁹ M. H. Kelsey,⁶⁹ P. Kim,⁶⁹ D. W. G. S. Leith,⁶⁹ S. Li,⁶⁹ S. Luitz,⁶⁹ V. Luth,⁶⁹ H. L. Lynch,⁶⁹ D. B. MacFarlane,⁶⁹ H. Marsiske,⁶⁹ R. Messner,⁶⁹ D. R. Muller,⁶⁹ C. P. O'Grady,⁶⁹ V. E. Ozcan,⁶⁹ A. Perazzo,⁶⁹ M. Perl,⁶⁹ T. Pulliam,⁶⁹ B. N. Ratcliff,⁶⁹ A. Roodman,⁶⁹ A. A. Salnikov,⁶⁹ R. H. Schindler,⁶⁹ J. Schwiening,⁶⁹ A. Snyder,⁶⁹ J. Stelzer,⁶⁹ D. Su,⁶⁹ M. K. Sullivan,⁶⁹ K. Suzuki,⁶⁹ S. K. Swain,⁶⁹ J. M. Thompson,⁶⁹ J. Va'vra,⁶⁹ N. van Bakel,⁶⁹ M. Weaver,⁶⁹ A. J. R. Weinstein,⁶⁹ W. J. Wisniewski,⁶⁹ M. Wittgen,⁶⁹ D. H. Wright,⁶⁹ A. K. Yarritu,⁶⁹ K. Yi,⁶⁹ C. C. Young,⁶⁹ P. R. Burchat,⁷⁰ A. J. Edwards,⁷⁰ S. A. Majewski,⁷⁰ B. A. Petersen,⁷⁰ C. Roat,⁷⁰ L. Wilden,⁷⁰ S. Ahmed,⁷¹ M. S. Alam,⁷¹ R. Bula,⁷¹ J. A. Ernst,⁷¹ V. Jain,⁷¹ B. Pan,⁷¹ M. A. Saeed,⁷¹ F. R. Wappeler,⁷¹ S. B. Zain,⁷¹ W. Bugg,⁷² M. Krishnamurthy,⁷² S. M. Spanier,⁷² R. Eckmann,⁷³ J. L. Ritchie,⁷³ A. Satpathy,⁷³ C. J. Schilling,⁷³ R. F. Schwitters,⁷³ J. M. Izen,⁷⁴ X. C. Lou,⁷⁴ S. Ye,⁷⁴ F. Bianchi,⁷⁵ F. Gallo,⁷⁵ D. Gamba,⁷⁵ M. Bomben,⁷⁶ L. Bosisio,⁷⁶ C. Cartaro,⁷⁶ F. Cossutti,⁷⁶ G. Della Ricca,⁷⁶ S. Dittongo,⁷⁶ L. Lanceri,⁷⁶ L. Vitale,⁷⁶ V. Azzolini,⁷⁷ N. Lopez-March,⁷⁷ F. Martinez-Vidal,⁷⁷ Sw. Banerjee,⁷⁸ B. Bhuyan,⁷⁸ C. M. Brown,⁷⁸ D. Fortin,⁷⁸ K. Hamano,⁷⁸ R. Kowalewski,⁷⁸ I. M. Nugent,⁷⁸ J. M. Roney,⁷⁸ R. J. Sobie,⁷⁸ J. J. Back,⁷⁹ P. F. Harrison,⁷⁹ T. E. Latham,⁷⁹ G. B. Mohanty,⁷⁹ M. Pappagallo,⁷⁹ H. R. Band,⁸⁰ X. Chen,⁸⁰ B. Cheng,⁸⁰ S. Dasu,⁸⁰ M. Datta,⁸⁰ K. T. Flood,⁸⁰ J. J. Hollar,⁸⁰ P. E. Kutter,⁸⁰ B. Mellado,⁸⁰ A. Mihalyi,⁸⁰ Y. Pan,⁸⁰ M. Pierini,⁸⁰ R. Prepost,⁸⁰ S. L. Wu,⁸⁰ Z. Yu,⁸⁰ and H. Neal⁸¹

(The BABAR Collaboration)

¹Laboratoire de Physique des Particules, IN2P3/CNRS et Université de Savoie, F-74941 Annecy-Le-Vieux, France

²Universitat de Barcelona, Facultat de Fisica, Departament ECM, E-08028 Barcelona, Spain

³Università di Bari, Dipartimento di Fisica and INFN, I-70126 Bari, Italy

⁴Institute of High Energy Physics, Beijing 100039, China

⁵University of Bergen, Institute of Physics, N-5007 Bergen, Norway

⁶Lawrence Berkeley National Laboratory and University of California, Berkeley, California 94720, USA

⁷University of Birmingham, Birmingham, B15 2TT, United Kingdom

⁸Ruhr Universität Bochum, Institut für Experimentalphysik 1, D-44780 Bochum, Germany

⁹University of Bristol, Bristol BS8 1TL, United Kingdom

¹⁰University of British Columbia, Vancouver, British Columbia, Canada V6T 1Z1

¹¹Brunel University, Uxbridge, Middlesex UB8 3PH, United Kingdom

¹²Budker Institute of Nuclear Physics, Novosibirsk 630090, Russia

¹³University of California at Irvine, Irvine, California 92697, USA

¹⁴University of California at Los Angeles, Los Angeles, California 90024, USA

¹⁵University of California at Riverside, Riverside, California 92521, USA

¹⁶University of California at San Diego, La Jolla, California 92093, USA

¹⁷University of California at Santa Barbara, Santa Barbara, California 93106, USA

¹⁸University of California at Santa Cruz, Institute for Particle Physics, Santa Cruz, California 95064, USA

¹⁹California Institute of Technology, Pasadena, California 91125, USA

²⁰University of Cincinnati, Cincinnati, Ohio 45221, USA

²¹University of Colorado, Boulder, Colorado 80309, USA

- ²²Colorado State University, Fort Collins, Colorado 80523, USA
²³Universität Dortmund, Institut für Physik, D-44221 Dortmund, Germany
²⁴Technische Universität Dresden, Institut für Kern- und Teilchenphysik, D-01062 Dresden, Germany
²⁵Laboratoire Leprince-Ringuet, CNRS/IN2P3, Ecole Polytechnique, F-91128 Palaiseau, France
²⁶University of Edinburgh, Edinburgh EH9 3JZ, United Kingdom
²⁷Università di Ferrara, Dipartimento di Fisica and INFN, I-44100 Ferrara, Italy
²⁸Laboratori Nazionali di Frascati dell'INFN, I-00044 Frascati, Italy
²⁹Università di Genova, Dipartimento di Fisica and INFN, I-16146 Genova, Italy
³⁰Harvard University, Cambridge, Massachusetts 02138, USA
³¹Universität Heidelberg, Physikalisches Institut, Philosophenweg 12, D-69120 Heidelberg, Germany
³²Imperial College London, London, SW7 2AZ, United Kingdom
³³University of Iowa, Iowa City, Iowa 52242, USA
³⁴Iowa State University, Ames, Iowa 50011-3160, USA
³⁵Johns Hopkins University, Baltimore, Maryland 21218, USA
³⁶Universität Karlsruhe, Institut für Experimentelle Kernphysik, D-76021 Karlsruhe, Germany
³⁷Laboratoire de l'Accélérateur Linéaire, IN2P3/CNRS et Université Paris-Sud 11, Centre Scientifique d'Orsay, B.P. 34, F-91898 ORSAY Cedex, France
³⁸Lawrence Livermore National Laboratory, Livermore, California 94550, USA
³⁹University of Liverpool, Liverpool L69 7ZE, United Kingdom
⁴⁰Queen Mary, University of London, E1 4NS, United Kingdom
⁴¹University of London, Royal Holloway and Bedford New College, Egham, Surrey TW20 0EX, United Kingdom
⁴²University of Louisville, Louisville, Kentucky 40292, USA
⁴³University of Manchester, Manchester M13 9PL, United Kingdom
⁴⁴University of Maryland, College Park, Maryland 20742, USA
⁴⁵University of Massachusetts, Amherst, Massachusetts 01003, USA
⁴⁶Massachusetts Institute of Technology, Laboratory for Nuclear Science, Cambridge, Massachusetts 02139, USA
⁴⁷McGill University, Montréal, Québec, Canada H3A 2T8
⁴⁸Università di Milano, Dipartimento di Fisica and INFN, I-20133 Milano, Italy
⁴⁹University of Mississippi, University, Mississippi 38677, USA
⁵⁰Université de Montréal, Physique des Particules, Montréal, Québec, Canada H3C 3J7
⁵¹Mount Holyoke College, South Hadley, Massachusetts 01075, USA
⁵²Università di Napoli Federico II, Dipartimento di Scienze Fisiche and INFN, I-80126, Napoli, Italy
⁵³NIKHEF, National Institute for Nuclear Physics and High Energy Physics, NL-1009 DB Amsterdam, The Netherlands
⁵⁴University of Notre Dame, Notre Dame, Indiana 46556, USA
⁵⁵Ohio State University, Columbus, Ohio 43210, USA
⁵⁶University of Oregon, Eugene, Oregon 97403, USA
⁵⁷Università di Padova, Dipartimento di Fisica and INFN, I-35131 Padova, Italy
⁵⁸Laboratoire de Physique Nucléaire et de Hautes Energies, IN2P3/CNRS, Université Pierre et Marie Curie-Paris6, Université Denis Diderot-Paris7, F-75252 Paris, France
⁵⁹University of Pennsylvania, Philadelphia, Pennsylvania 19104, USA
⁶⁰Università di Perugia, Dipartimento di Fisica and INFN, I-06100 Perugia, Italy
⁶¹Università di Pisa, Dipartimento di Fisica, Scuola Normale Superiore and INFN, I-56127 Pisa, Italy
⁶²Prairie View A&M University, Prairie View, Texas 77446, USA
⁶³Princeton University, Princeton, New Jersey 08544, USA
⁶⁴Università di Roma La Sapienza, Dipartimento di Fisica and INFN, I-00185 Roma, Italy
⁶⁵Universität Rostock, D-18051 Rostock, Germany
⁶⁶Rutherford Appleton Laboratory, Chilton, Didcot, Oxon, OX11 0QX, United Kingdom
⁶⁷DSM/Dapnia, CEA/Saclay, F-91191 Gif-sur-Yvette, France
⁶⁸University of South Carolina, Columbia, South Carolina 29208, USA
⁶⁹Stanford Linear Accelerator Center, Stanford, California 94309, USA
⁷⁰Stanford University, Stanford, California 94305-4060, USA
⁷¹State University of New York, Albany, New York 12222, USA
⁷²University of Tennessee, Knoxville, Tennessee 37996, USA
⁷³University of Texas at Austin, Austin, Texas 78712, USA
⁷⁴University of Texas at Dallas, Richardson, Texas 75083, USA
⁷⁵Università di Torino, Dipartimento di Fisica Sperimentale and INFN, I-10125 Torino, Italy
⁷⁶Università di Trieste, Dipartimento di Fisica and INFN, I-34127 Trieste, Italy
⁷⁷IFIC, Universitat de València-CSIC, E-46071 Valencia, Spain
⁷⁸University of Victoria, Victoria, British Columbia, Canada V8W 3P6
⁷⁹Department of Physics, University of Warwick, Coventry CV4 7AL, United Kingdom
⁸⁰University of Wisconsin, Madison, Wisconsin 53706, USA
⁸¹Yale University, New Haven, Connecticut 06511, USA

(Dated: October 17, 2018)

We measure the branching fraction (\mathcal{B}), polarization (f_L) and CP asymmetry (A_{CP}) of $B^\pm \rightarrow \rho^\pm \rho^0$ decays and search for the decay $B^\pm \rightarrow \rho^\pm f_0(980)$ based on a data sample of 231.8 million $\Upsilon(4S) \rightarrow B\bar{B}$ decays collected with the *BABAR* detector at the SLAC PEP-II asymmetric-energy B factory. In $B^\pm \rightarrow \rho^\pm \rho^0$ decays we measure $\mathcal{B} = (16.8 \pm 2.2 \pm 2.3) \times 10^{-6}$, $f_L = 0.905 \pm 0.042^{+0.023}_{-0.027}$, and $A_{CP} = -0.12 \pm 0.13 \pm 0.10$, and find an upper limit on the branching fraction of $B^\pm \rightarrow \rho^\pm f_0(980)(\rightarrow \pi^+ \pi^-)$ decays of 1.9×10^{-6} at 90% confidence level.

PACS numbers: 13.25.Hw, 12.15.Hh, 11.30.Er

The measurement of the CP -violating phase of the Cabibbo-Kobayashi-Maskawa (CKM) quark-mixing matrix [1] is an important part of the present program in particle physics. Violation of CP symmetry is manifested as a non-zero area of the CKM unitarity triangle [2]. In this paper we report the measurement of the branching fraction, polarization and CP asymmetry of the $B^\pm \rightarrow \rho^\pm \rho^0$ decay mode, which is needed for the $\rho\rho$ isospin analysis used to extract $\alpha = \arg[-V_{td}V_{tb}^*/V_{ud}V_{ub}^*]$ [3]. We also set an upper limit on the unknown branching fraction of $B^\pm \rightarrow \rho^\pm f_0(980)(\rightarrow \pi^+ \pi^-)$, which is measured to control this background to the $B^\pm \rightarrow \rho^\pm \rho^0$ analysis.

In $B^0(\bar{B}^0) \rightarrow \rho^+ \rho^-$ decays [4] the interference between the $B\bar{B}$ oscillations which depend on V_{td} and the dominating tree-level amplitude $b \rightarrow u\bar{u}d$ causes a time-dependent CP asymmetry that depends on $\sin(2\alpha)$. The presence of loop (penguin) amplitudes leads to a shift $\delta\alpha = |\alpha - \alpha_{\text{eff}}^{\rho\rho}|$, between the physical weak phase α , and the effective one $\alpha_{\text{eff}}^{\rho\rho}$, experimentally measured in $B^0 \rightarrow \rho^+ \rho^-$ decays [5, 6]. However, the penguin amplitudes in these decays are known to contribute at a very low level due to the small upper limit of 1.1×10^{-6} at 90% confidence level (CL) [7], obtained from the branching fraction of the penguin dominated mode $B^0 \rightarrow \rho^0 \rho^0$. The size of $\delta\alpha$ can be extracted from the full isospin analysis combining all $B \rightarrow \rho\rho$ modes [3].

In $B \rightarrow \rho\rho$ decays, a spin zero particle decays into two spin one particles. The final state is therefore a superposition of two transversely polarized modes (helicity ± 1) and one longitudinal mode (helicity 0), which can be measured through an angular analysis. The longitudinal polarization fraction f_L is defined as the fraction of decays to the helicity zero state, $f_L = \Gamma_L/\Gamma$, where Γ is the total decay rate and Γ_L is the decay rate to the longitudinally polarized final state. The transverse polarization is a mixed CP state while the longitudinal state is pure CP even. The previous measurements of f_L [8, 9] showed the decay is consistent with being fully longitudinally polarized.

Our analysis is performed in the helicity frame [10] as a function of the two helicity angles θ_\pm and θ_0 where the helicity angle of a ρ^\pm (ρ^0) meson is defined as the angle between its daughter π^\pm (π^+) and the direction opposite to the B meson in the ρ^\pm (ρ^0) rest frame. The polarization f_L can be extracted from the differential decay

rate:

$$\frac{1}{\Gamma} \frac{d^2\Gamma}{d\cos\theta_\pm d\cos\theta_0} = \frac{9}{4} \left[f_L \cos^2\theta_\pm \cos^2\theta_0 + \frac{1}{4}(1-f_L) \sin^2\theta_\pm \sin^2\theta_0 \right]. \quad (1)$$

Here we integrate over the angle between the ρ -meson decay planes.

The measurements presented in this paper are based on data collected with the *BABAR* detector [11] at the SLAC PEP-II asymmetric-energy e^+e^- collider. The analyzed data sample of 231.8 ± 2.6 million $B\bar{B}$ pairs produced at the $\Upsilon(4S)$ resonance corresponds to an integrated luminosity of 210.5 fb^{-1} .

To reconstruct $B^\pm \rightarrow \rho^\pm \rho^0$ and $B^\pm \rightarrow \rho^\pm f_0$ decays, we select events with at least three charged tracks and one neutral pion candidate. Charged tracks are required to originate from the interaction point and have particle identification information inconsistent with kaon, electron, and proton hypotheses. We form $\pi^0 \rightarrow \gamma\gamma$ candidates from pairs of calorimeter showers, each with a photon-like lateral spread and a minimum energy of 50 MeV. The invariant mass of π^0 candidates is required to fall in the range $0.10 < m_{\gamma\gamma} < 0.16 \text{ GeV}/c^2$.

The mass of charged ρ^\pm candidates must satisfy $0.396 < m_{\pi^\pm \pi^0} < 1.146 \text{ GeV}/c^2$ where the low-side requirement on the $\pi^\pm \pi^0$ mass is chosen to exclude $K_S^0 \rightarrow \pi^+ \pi^-$ decays. Neutral final state meson candidates (ρ^0, f_0) must satisfy $0.520 < m_{\pi^+ \pi^-} < 1.146 \text{ GeV}/c^2$. In order to suppress backgrounds with low momentum pions, the helicity angles are required to fall in the ranges $-0.8 < \cos\theta_\pm < 0.95$ and $|\cos\theta_0| < 0.95$. Backgrounds from $D^0 \rightarrow K^-\pi^+\pi^0$ and $D^0 \rightarrow \pi^-\pi^+\pi^0$ decays are reduced by requiring the candidate D^0 invariant mass to be at least $40 \text{ MeV}/c^2$ away from the D^0 mass.

About 20% of the selected events have multiple B candidates and the one that has the reconstructed π^0 mass closest to the π^0 mass is kept. In the case that more than one candidate has the same reconstructed π^0 mass, we select one at random.

Continuum decays represent the largest source of background and are reduced by requiring $|\cos\theta_T| < 0.8$, where θ_T is the cosine of the angle between the B thrust axis and that from the rest of the event (ROE). To further discriminate signal from continuum, we also use a neural network built out of five event-shape variables: a Fisher discriminant combining the 0th and 2nd order monomials

[12] for charged particles and neutral clusters of the ROE; the cosine of the angle between the direction of the B and the collision axis (z) in the center-of-mass (CM) frame; the cosine of the angle between the B thrust axis and the z axis; the variable $|\cos\theta_T|$ defined above; and the sum of transverse momenta in the ROE relative to the z axis. The output is transformed into a variable x_{NN} which has roughly Gaussian signal and background distributions. We select candidates in a range of x_{NN} that removes 54% of continuum background events while retaining 90% of the signal. After these selections, about 85% of the remaining events are from continuum decays.

Signal event candidates are further identified based on two kinematic variables: the beam-energy-substituted mass $m_{ES} = \sqrt{(s/2 + \mathbf{p}_i \cdot \mathbf{p}_B)^2/E_i^2 - \mathbf{p}_B^2}$, using the total initial e^+e^- 4-momentum (E_i, \mathbf{p}_i), CM energy (\sqrt{s}) and the B momentum (\mathbf{p}_B), and $\Delta E = E_B^* - \sqrt{s}/2$, the difference between the reconstructed B energy in the CM frame (E_B^*) and the beam energy. Events are selected if $m_{ES} > 5.26 \text{ GeV}/c^2$ and $|\Delta E| < 150 \text{ MeV}$.

After the selection criteria are applied, the efficiency is 8.4% for longitudinal and 18.6% for transverse polarized $B^\pm \rightarrow \rho^\pm \rho^0$ decays. The selection efficiency is 16.6% for $B^\pm \rightarrow \rho^\pm f_0$ decays. Any possible interference effects between the $B^\pm \rightarrow \rho^\pm \rho^0$ and $B^\pm \rightarrow \rho^\pm f_0$ are neglected.

An unbinned extended maximum likelihood fit is applied to the selected sample of $N_{\text{tot}} = 74293$ events in order to measure the $B^\pm \rightarrow \rho^\pm \rho^0$ event yield, polarization, and charge asymmetry as well as the $B^\pm \rightarrow \rho^\pm f_0$ event yield. The likelihood function is:

$$\mathcal{L} = \frac{1}{N_{\text{tot}}!} \exp \left(-\sum_{k=1}^M n_k \right) \prod_{i=1}^{N_{\text{tot}}} \left(\sum_{j=1}^M n_j \mathcal{P}_j(\vec{x}_i) \right), \quad (2)$$

where M is the number of hypotheses (signal, misreconstructed signal, continuum and B -background classes), and n_k (n_j) represents the number of measured events for each hypothesis determined by maximizing the likelihood function. $\mathcal{P}_j(\vec{x}_i)$ is the product of the probability density functions (PDFs) of hypothesis j evaluated at the i -th event's measured variables, $\vec{x}_i = \{m_{ES}, \Delta E, m_{\pi^\pm \pi^0}, m_{\pi^+ \pi^-}, \cos\theta_\pm, \cos\theta_0, x_{NN}\}$. In addition, the charge asymmetry, obtained from the measured B^- and B^+ signal candidate decay yields, $A_{CP} = \frac{N_{B^-} - N_{B^+}}{N_{B^-} + N_{B^+}}$, is determined in the fit to the data.

Each discriminating variable in the likelihood function is modeled with a PDF extracted either from the data, or from high statistics Monte Carlo (MC) simulated data samples. The correlations between the variables are assumed to be small and the PDFs independent. This is checked with systematic error studies, and corrections are applied where necessary.

The continuum background ΔE , m_{ES} , and x_{NN} distributions are modeled with one-dimensional parameterized distributions taken from fits to the data. Correlations

are observed between the $m_{\pi\pi}$ and $\cos\theta$ distributions for both ρ -meson candidates, which are taken into account with two-dimensional PDFs. The signal component is modeled with one-dimensional parameterized distributions for each of six variables; m_{ES} is modeled with a non-parametric PDF [13]. The signal PDF shapes are obtained from fits to signal MC sample after the selection is applied. Events with a true $B^\pm \rightarrow \rho^\pm \rho^0$ decay but with wrong tracks or calorimeter clusters assigned to the final state are referred to as self cross feed (SCF) events. They make up 35% and 14% of the selected longitudinally and transversely polarized signal samples, respectively. The longitudinal and transverse SCF components and B -background PDFs are determined in a similar manner using high statistics MC samples and modeled with non-parametric PDFs [13] for each variable.

To understand the backgrounds from other B decay modes we use MC simulated events. There are two types of B -background: ‘charmed’ (decays involving $b \rightarrow c$ transitions), and ‘charmless’ (all other b decays). Altogether sixteen B -background categories plus the two SCF components are included in the fit. The SCF yields and polarization are fixed in the final fit at values that match those fitted for the signal in previous iterations of the fit. Four specific charmed background modes are included: $B^- \rightarrow D^0 \pi^-$, $B^- \rightarrow D^0 \rho^-$, $B^- \rightarrow D^{*0} \pi^-$, and $B^- \rightarrow D^{*0} \rho^-$. Other charmed backgrounds are combined into two generic classes of events for charged and neutral charmed B decays. For the charmless B -backgrounds, separate MC samples of eight modes were used: neutral B decaying to $\rho^+ \rho^-$ and charged B decaying to $\rho^\pm f_0(980)$, $\eta' \rho^\pm$, $K^{*0} \rho^\pm$, $a_1^0 \pi^\pm$, $a_1^\pm \pi^0$, $a_1^\pm \rho^0$, and $a_1^0 \rho^\pm$ with the decays $a_1^0 \rightarrow (\rho\pi)^0$ and $a_1^\pm \rightarrow (\rho\pi)^\pm$. For B decaying to vector-mesons, only the longitudinal component of the decay is considered. Two generic categories, one for 5-body modes and one for all ‘other charmless’ decays, complete the B -background model.

The number of ‘other charmless’ events and the $B^\pm \rightarrow \rho^\pm f_0$ yield were determined from the data fit. The other fourteen backgrounds had their yields fixed in the fit. We use the following branching fractions:

$$\begin{aligned} \mathcal{B}(B^0 \rightarrow \rho^+ \rho^-) &= (26.2 \pm 3.7) \times 10^{-6} & [14], \\ \mathcal{B}(B^\pm \rightarrow \eta' \rho^\pm) &= (12.9 \pm 6.5) \times 10^{-6} & [15], \\ \mathcal{B}(\eta' \rightarrow \rho^0 \gamma) &= 0.295 \pm 0.010 & [16], \\ \mathcal{B}(B^+ \rightarrow K^{*0} \rho^+) &= (10.5 \pm 1.8) \times 10^{-6} & [14], \\ &\text{and } \mathcal{B}(K^{*0} \rightarrow K^+ \pi^-) = 2/3. \end{aligned}$$

The decays $B^\pm \rightarrow (a_1 \pi)^\pm$ and $B^\pm \rightarrow (a_1 \rho)^\pm$ have few experimental constraints [17, 18]. We adopt the following B^\pm branching ratios, in units of 10^{-6} , and assume a 100% systematic uncertainty: $a_1^0 \pi^+ = 12$, $a_1^+ \pi^0 = 6$, $a_1^0 \rho^+ = a_1^+ \rho^0 = 48$.

Table I shows the results of the fit, where the quoted errors are statistical errors only. Projection plots for m_{ES} and ΔE are shown in Fig. 1.

Systematic effects are considered in the modeling of

TABLE I: Summary of the results of the fit with statistical errors (before correction for fit biases).

Observables	Fitted value
$B^\pm \rightarrow \rho^\pm \rho^0$ yield	390 ± 49 events
Polarization f_L	0.897 ± 0.042
Charge asymmetry A_{CP}	-0.12 ± 0.13
$B^\pm \rightarrow \rho^\pm f_0$ yield	51 ± 30 events

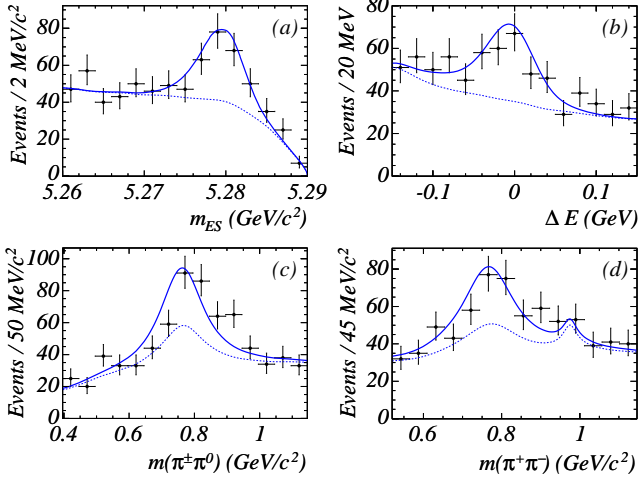


FIG. 1: Projections of (a) m_{ES} , (b) ΔE , (c) $m_{\pi^\pm \pi^0}$, and (d) $m_{\pi^+ \pi^-}$ with a cut on the ratio of the signal and background likelihoods that selects about 40% of the signal. For (a) and (b), the observable plotted is excluded from the fit in calculating the likelihood used for the enrichment selection. For (c) and (d), only the m_{ES} , ΔE , and x_{NN} variables have been used in calculating the likelihood. Points represent on-resonance data, dashed lines the continuum and $B\bar{B}$ backgrounds PDFs, and solid lines the likelihood function with yields taken from the fit were all variables have been used.

the PDF shapes and biases in the fit model. Tests of the fit are made by using a large number of MC samples containing the amounts of signal, continuum and B -background events measured or fixed in the data fit. The fits to these samples should reproduce the number of MC events modeled. A shift of the fitted values with respect to the generated ones indicates a bias in the fitting procedure, for which a correction to the yield is then applied. We use the same technique to study the effects of correlations between the neural net and helicity variables in the $q\bar{q}$ continuum. No other significant correlations were observed between the other discriminating variables. After combining these two effects we find an intrinsic bias in the fit of $+25 \pm 27$ on the number of $B^\pm \rightarrow \rho^\pm \rho^0$ events, -0.008 ± 0.005 on f_L and $+23.6 \pm 9.8$ events on the $B^\pm \rightarrow \rho^\pm f_0$ yield. These biases are corrected from the fit measurements, and half of each separate fit bias is taken as the systematic error.

Many of the B -background rates are poorly known.

The effect of uncertainties in these values is evaluated by varying the number of events in each background category within the range allowed by the error on the branching fraction. Fourteen non-resonant backgrounds that are not in the default fit are tested by adding them singly to the fit with a yield that is allowed to vary. The only shift seen was associated with the mode $B^\pm \rightarrow \pi^\pm \pi^0 \pi^0$, and is taken as a symmetric systematic uncertainty.

The systematic error associated with misreconstructed signal is evaluated by taking the difference between the default fit and the one for which these events are not modeled, and therefore mostly absorbed into the ‘other charmless’ background category. We consider the error due to the uncertainty on the signal, B -background, and continuum PDF shapes and estimate a systematic error by varying these shapes within their statistical uncertainty. The impact of the uncertainty on the measurement of the f_0 mass and width [19] has also been evaluated. The values of the systematic errors described above are given in Table II.

TABLE II: Summary of the systematic uncertainties on the $B^\pm \rightarrow \rho^\pm \rho^0$ yield, the polarization f_L , and the $B^\pm \rightarrow \rho^\pm f_0$ yield.

Source	$\rho^\pm \rho^0$ yield	f_L	$\rho^\pm f_0$ yield
Fit bias	27.3	0.005	9.8
B -background rates	11.0	0.007	2.8
Non-resonant backgrounds	12.0	0.009	3.0
Amount of SCF	24.0	0.010	0.6
PDF shapes	$+21.1$ -22.5	$+0.017$ -0.022	$+7.9$ -13.5
f_0 mass and width	$+0.9$ -0.6	0.000	3.9
Total	$+45$ -46	$+0.023$ -0.027	$+14$ -18

Systematic uncertainties in the reconstruction and calibration procedure introduce a systematic error of 3% after a correction of -2.5% on the π^0 reconstruction efficiency, 3.9% after a correction of -1.5% on the track reconstruction efficiency, and a systematic error of 1.1% from the particle identification. The uncertainty on the efficiency ratio between longitudinal and transverse events is found to be negligible. The error on A_{CP} includes a 0.45% uncertainty in the charged track reconstruction asymmetry, a 4% uncertainty from the detector’s intrinsic charged particle identification asymmetry, and a 9% uncertainty which is the largest single shift obtained when assuming a uniform probability for the charge asymmetry of every B -background individually.

In summary, we measure the branching fraction, longitudinal polarization, and CP asymmetry of the decay $B^\pm \rightarrow \rho^\pm \rho^0$, using a dataset of about 231.8 million $B\bar{B}$ pairs, to be:

$$\begin{aligned} \mathcal{B}(B^\pm \rightarrow \rho^\pm \rho^0) &= (16.8 \pm 2.2 \pm 2.3) \times 10^{-6}, \\ f_L(B^\pm \rightarrow \rho^\pm \rho^0) &= 0.905 \pm 0.042^{+0.023}_{-0.027}, \\ A_{CP}(B^\pm \rightarrow \rho^\pm \rho^0) &= -0.12 \pm 0.13 \pm 0.10. \end{aligned}$$

The measurement of the branching fraction has improved by a factor of about two with respect to the previous *BABAR* measurement [8], and supersedes it. The isospin relations between branching ratios are consistent between this measurement and those of $\rho^+ \rho^-$ and $\rho^0 \rho^0$ [14], validating the approach [3] used to constraint α . Moreover, our measurements confirm that this mode is largely longitudinally polarized. They also confirm that the charge asymmetry is consistent with zero as expected for decays proceeding through one decay channel only; this suggests the contributions of electroweak penguins are small in the $B \rightarrow \rho\rho$ system.

In addition we measure $\mathcal{B}(B^\pm \rightarrow \rho^\pm f_0(980)(\rightarrow \pi^+ \pi^-)) = (0.7 \pm 0.8 \pm 0.5) \times 10^{-6}$ with a significance of 0.4σ . We set an upper limit on the branching fraction of 1.9×10^{-6} at 90% confidence level by finding the yield (N) that satisfies $\int_0^N \mathcal{L}(n)dn / \int_0^\infty \mathcal{L}(n)dn = 0.9$ taking into account systematic uncertainties.

We are grateful for the excellent luminosity and machine conditions provided by our PEP-II colleagues, and for the substantial dedicated effort from the computing organizations that support *BABAR*. The collaborating institutions wish to thank SLAC for its support and kind hospitality. This work is supported by DOE and NSF (USA), NSERC (Canada), IHEP (China), CEA and CNRS-IN2P3 (France), BMBF and DFG (Germany), INFN (Italy), FOM (The Netherlands), NFR (Norway), MIST (Russia), and PPARC (United Kingdom). Individuals have received support from the Marie Curie EIF (European Union) and the A. P. Sloan Foundation.

-
- [†] Also with Università della Basilicata, Potenza, Italy
- [1] N. Cabibbo, Phys. Rev. Lett. **10**, 531 (1963);
M. Kobayashi and T. Maskawa, Prog. Theor. Phys. **49**, 652 (1973).
 - [2] C. Jarlskog, Phys. Rev. Lett. **55**, 1039 (1985).
 - [3] M. Gronau and D. London, Phys. Rev. Lett. **65**, 3381 (1990).
 - [4] Charge conjugation is implied throughout this document, unless explicitly stated.
 - [5] *BABAR* Collaboration, B. Aubert *et al.*, Phys. Rev. Lett. **95**, 041805 (2005).
 - [6] *Belle* Collaboration, A. Somov *et al.*, Phys. Rev. Lett. **96**, 171801 (2006).
 - [7] *BABAR* Collaboration, B. Aubert *et al.*, Phys. Rev. Lett. **94**, 131801 (2005).
 - [8] *BABAR* Collaboration, B. Aubert *et al.*, Phys. Rev. Lett. **91**, 171802 (2003).
 - [9] *Belle* Collaboration, J. Zhang *et al.*, Phys. Rev. Lett. **91**, 221801 (2003).
 - [10] G. Kramer and W. F. Palmer, Phys. Rev. **D 45**, 193 (1992).
 - [11] *BABAR* Collaboration, B. Aubert *et al.*, Nucl. Instr. Methods Phys. Res., Sect. C **A479**, 1 (2002).
 - [12] *BABAR* Collaboration, B. Aubert *et al.*, Phys. Rev. Lett. **89**, 281802 (2002).
 - [13] K. S. Cranmer, Comput. Phys. Commun. **136**, 198 (2001).
 - [14] Heavy Flavor Averaging Group (HFAG), hep-ex/0603003.
 - [15] *BABAR* Collaboration, B. Aubert *et al.*, Phys. Rev. **D 70**, 032006 (2004).
 - [16] S. Eidelman *et al.*, Phys. Lett. B **592**, 1 (2004).
 - [17] *BABAR* Collaboration, B. Aubert *et al.*, hep-ex/0603050 (SLAC-PUB-11769).
 - [18] *BABAR* Collaboration, B. Aubert *et al.*, hep-ex/0605024 (SLAC-PUB-11850).
 - [19] E791 Collaboration, E. M. Aitala *et al.*, Phys. Rev. Lett. **86**, 765 (2004).

* Also with Università di Perugia, Dipartimento di Fisica, Perugia, Italy

We measure the branching fraction (\mathcal{B}), polarization (f_L) and CP asymmetry (A_{CP}) of $B^\pm \rightarrow \rho^\pm \rho^0$ decays and search for the decay $B^\pm \rightarrow \rho^\pm f_0(980)$ based on a data sample of 231.8 million $\Upsilon(4S) \rightarrow B\bar{B}$ decays collected with the BaBar detector at the SLAC PEP-II asymmetric-energy B factory. In $B^\pm \rightarrow \rho^\pm \rho^0$ decays we measure $\mathcal{B} = (16.8 \pm 2.2 \pm 2.3) \times 10^{-6}$, $f_L = 0.905 \pm 0.042^{+0.023}_{-0.027}$, and $A_{CP} = -0.12 \pm 0.13 \pm 0.10$, and find an upper limit on the branching fraction of $B^\pm \rightarrow \rho^\pm f_0(980) (\rightarrow \pi^+ \pi^-)$ decays of 1.9×10^{-6} at 90% confidence level.